Organometallic Intermediates in the Controlled Radical Polymerization of Styrene by α-Diimine Iron Catalysts

Michael P. Shaver, Laura E. N. Allan, and Vernon C. Gibson*

Department of Chemistry, Imperial College, Exhibition Road, South Kensington, London, SW7 2AZ, U.K.

Received April 24, 2007

The α-diimine iron complexes $^{R',R''}[N,N]FeCl_2$ ($^{R',R''}[N,N] = R'{-}N{=}CR''{-}CR''{=}N{-}R'$) are efficient catalysts for the atom-transfer radical polymerization (ATRP) of styrene when R′ and R″ are electron-donating substituents and favor catalytic chain transfer (CCT) when electron-withdrawing substituents are employed. An organometallic pathway, alongside a halogen-atom-transfer equilibrium, is proposed to mediate the observed reactivity. The model alkyl complexes, $^{R',R''}[N,N]FeCl_2(R)$, where R = $PhCH_2$ and Ph(Me)CH, were generated via treatment of $^{R',R''}[N,N]FeCl_3$ with RMgCl. The alkyl derivatives obtained from intermediate spin-state $^{R',R''}[N,N]FeCl_3$ complexes were found to be stable to ca. −30 °C and favor CCT, whereas the alkyl derivatives derived from high-spin-state trichloride precursors are unstable above −78 °C and favor ATRP. Azo-initiated polymerizations of styrene are moderately controlled by α-diimine iron catalysts. The role of organometallic-mediated radical polymerization (OMRP) in the controlled polymerization of styrene is discussed: an analysis of the radical concentrations generated by the competing OMRP and ATRP equilibria indicates that the halogenophilicity of the Fe(II) catalyst dominates the carbophilic alkyl radical-trapping capacity of the Fe(II) species in this α-diimine catalyst system.

Introduction

The development of controlled/“living” radical polymerization reactions has provided a technologically important advance in synthetic polymer chemistry. Key milestones include the introduction of atom-transfer radical polymerization,[1,2] nitroxide-mediated radical polymerization,[3] and reversible addition−fragmentation chain transfer.[4,5] In each of these reactions control is achieved by the reversible deactivation of growing polymer chains, maintaining a low concentration of radicals.

In our own studies we have shown that α-diimine iron complexes $^{R',R''}[N,N]FeCl_2$ ($^{R',R''}[N,N] = R'{-}N{=}CR''{-}CR''{=}N{-}R'$) are able to mediate the polymerization of styrene either through an atom-transfer radical polymerization (ATRP) mechanism or via a catalytic chain-transfer (CCT) process.[6] Investigations into substituted α-diimine complexes through computational, reactivity, and mechanistic studies have indicated that this switch in polymerization mechanism correlates with a change in metal spin-state in the corresponding $^{R',R''}[N,N]FeCl_3$ complexes, with electron-withdrawing groups stabilizing intermediate spin-state ($S = 3/2$) complexes and electron-donating groups supporting high-spin ($S = 5/2$) Fe(III) species. It is proposed that these divergent reactivities arise as a consequence of the interplay of the ATRP and organometallic-mediated radical polymerization (OMRP) equilibria shown in Scheme 1.

Scheme 1. Possible Pathways for α-Diimine Iron-Mediated Radical Polymerization of Styrene

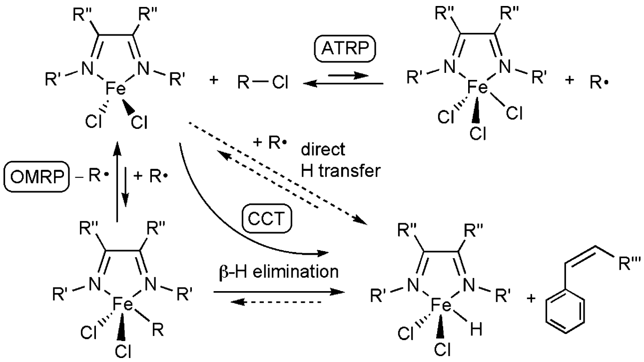

The halogen-atom transfer equilibrium established in ATRP affords chlorine-capped polymer chains, minimizing the concentration of radicals in solution and thus reducing bimolecular termination reactions. The degree of control via ATRP depends upon the propensity of the Fe(II) species to abstract a halogen atom from an alkyl halide initiator or propagating chain end, which can be viewed to be a function of the Fe(II) center’s *halogenophilicity*. The radicals present in solution can also be trapped by the Fe(II) complex to form a new Fe(III) organometallic species, establishing an OMRP equilibrium; the analogous idiom for the predilection of the Fe(II) species for a carbon-based radical can be termed its *carbophilicity*. Olefin-terminated polymer chains can then be generated via β-hydrogen elimination from this iron-alkyl species or, alternatively, through direct hydrogen transfer from the organoradical to the Fe(II) catalyst. From our studies to date, it has become apparent that ATRP or CCT products can be favored depending upon the relative halogenophilicity versus carbophilicity of these species which is determined by the effect of the imino or ligand backbone substituents on the spin-state of the iron centers.[6−8]

The role of OMRP in controlling the polymerization of styrene in this system is rather less well understood than the ATRP process. Transition metals, especially cobalt, have previously shown efficacy in controlling radical polymerizations

---

* Corresponding author. Fax: 020 7594 5810. Tel: 020 7594 5830. E-mail: v.gibson@imperial.ac.uk.

[1] Matyjaszewski, K.; Xia, J. *Chem. Rev.* **2001**, *101*, 2921.

[2] Kamigaito, M.; Ando, T.; Sawamoto, M. *Chem. Rev.* **2001**, *101*, 3689.

[3] Hawker, C. J.; Bosman, A. W.; Harth, E. *Chem. Rev.* **2001**, *101*, 3661.

[4] Favier, A.; Charreyre, M.-T. *Macromol. Rapid Commun.* **2006**, *27*, 653.

[5] Moad, G.; Rizzardo, E.; Thang, S. H. *Aust. J. Chem.* **2005**, *58*, 379.

[6] Shaver, M. P.; Allan, L. E. N.; Rzepa, H. S.; Gibson, V. C. *Angew. Chem., Int. Ed.* **2006**, *45*, 1241.

10.1021/om700395h CCC: $37.00

by an entirely organometallic pathway. This mechanism works on the same principles as a reversible addition−cleavage mechanism, with the transition metal acting as a reversible spin-trap. OMRP offers control over polymerizations based on the reversible homolytic cleavage of the weak bond between an alkyl group and a metal catalyst. Cobalt systems supported by judiciously chosen ligands have been shown to yield high molecular weight acrylate polymers with very low polydispersities ($M_w/M_n \approx 1.1$).[9,10] Recently this work has expanded to include the controlled polymerization of vinyl acetate. While Co(acac)$_2$ is unable to mediate the polymerization of acrylate monomers, it can effectively control the polymerization of vinyl acetate in bulk[11] and suspension[12] and has led to the development of end-functionalized[13] and block copolymers[14] of poly(vinyl acetate) and poly(vinyl alcohol).

A few systems have been reported to display both ATRP and OMRP behavior. The polymerization of styrene by the half-sandwich molybdenum compounds[15,16] CpMoCl$_2$(PMe$_3$)$_2$ and CpMoCl$_2$(dppe) proceed via ATRP, generating polystyrene with moderate polydispersities (PDIs) (ca. 1.5) and molecular weights that increase linearly with conversion. The same catalysts can also function in the OMRP of styrene, where the polymer molecular weights, though higher than those predicted on the basis of monomer to initiator ratios, increase linearly with conversion and have PDIs (1.3−1.7) indicative of controlled behavior. Other examples of catalysts that are capable of controlling polymerization through both ATRP and OMRP mechanisms include Cp$_2$TiCl$_2$[17,18] and OsCl$_2$(PPh$_3$)$_3$.[19] These findings suggest that, under ATRP conditions, the radical concentration is regulated not only by the atom-transfer equilibrium but also via the trapping of radicals by the lower oxidation state metal species. The interplay of these various one-electron processes has recently been reviewed.[20]

In an earlier study we detailed the synthesis, characterization, and styrene polymerization behavior of a family of 2,3-substituted α-diimine iron catalysts.[8] Electron-withdrawing substituents favor Fe(III) complexes with intermediate spin-states and generate low molecular weight vinylene-terminated products characteristic of a CCT mechanism. Electron-donating substituents, such as alkyl groups or 4-(dimethylamino)phenyl, favor Fe(III) complexes of high spin-state and generate halogen end-capped polymers via ATRP. Here, we report the results of our investigations into the capacity of $^{R',R''}$[*N*,*N*]FeCl$_2$ catalysts to engage in OMRP and a study of the factors that influence the mechanistic pathways, ATRP versus OMRP, followed in these reactions.

Scheme 2. Decomposition Pathways for $^{R',R''}$[*N*,*N*]FeCl$_2$Bn Complexes

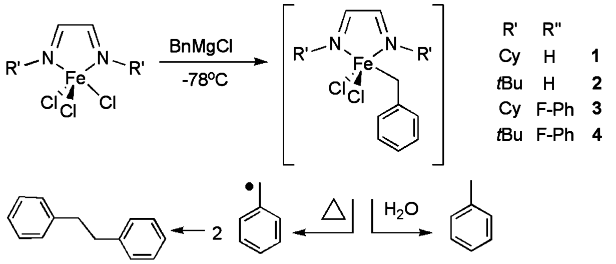

Results

Formation and Stability of Fe(III)-Alkyl Species. Our earlier studies have shown that incorporating electron-withdrawing groups at the 2,3 positions of α-diimine ligands promotes a switch in polymerization mechanism from ATRP to CCT.[6,8] This switch also correlates with a change in the spin-state of the parent Fe(III) complexes, from $S = 5/2$ to $S = 3/2$. But what effect does this spin-state change have on the stability and function of $^{R',R''}$[*N*,*N*]FeCl$_2$(P) intermediates in the polymerization?

In order to gain further understanding of the role of organometallic intermediates in these polymerization systems, the reactivity of a family of $^{R',R''}$[*N*,*N*]FeCl$_3$ (Scheme 2) complexes toward Grignard reagents was investigated. The stability of the product $^{R',R''}$[*N*,*N*]FeCl$_2$R complexes can provide an indication of the relative carbophilicity of the parent $^{R',R''}$[*N*,*N*]FeCl$_2$ catalysts. Initially, the mono-benzyl Fe(III) catalysts were targeted via treatment of $^{R',R''}$[*N*,*N*]FeCl$_3$ with BnMgCl (Bn = C$_6$H$_5$CH$_2$) at −78 °C. There are two possible decomposition pathways for the alkyl complexes so generated, as shown in Scheme 2. If the $^{R',R''}$[*N*,*N*]FeCl$_2$Bn is thermally unstable, then it would be anticipated to decompose by homolytic Fe−C bond cleavage to generate benzyl radicals, which can couple to give bibenzyl (Bn$_2$, PhCH$_2$CH$_2$Ph). If there is enhanced stability for the iron alkyl species, it will decompose at a higher temperature. Then, quenching the reaction with H$_2$O below its decomposition temperature would be expected to generate toluene via protonolysis of the Fe−C bond.

Addition of BnMgCl at −78 °C to the high-spin complex **1** produced an immediate color change from yellow to deep purple, and ^{Cy,H}[*N*,*N*]FeCl$_2$ was isolated from the reaction mixture. GC analysis of the reaction products indicated the formation of Bn$_2$ via the reductive alkylation of **1**. Similarly, alkylation of **2**, also a high-spin complex, produced Bn$_2$ at −78 °C. In both of these cases, the iron-alkyl species is unstable at −78 °C; the Fe−C bond cleaves homolytically to generate carbon radicals in solution, which couple to form Bn$_2$. The reaction of **3** and **4** with BnMgCl at −78 °C produced very different results. GC analysis of quenched aliquots showed that toluene (T) was the major product, not bibenzyl. As the solution was warmed to −30 °C, a red-brown to purple color change coincided with Bn$_2$ becoming the major decomposition product (Figure 1). Thus, it is apparent that radical coupling occurs at a higher temperature, implying that the Fe-alkyl complexes derived from **3** and **4** have improved stability. This corresponds

---

[7] While the term halogenophilicity has been previously employed to describe the reaction of a metal complex with a halide ion (see *Macromolecules* **2004**, 9768), the terms halogenophilicity and carbophilicity are used here to describe the relative predilection for a complex to form metal−halogen and metal−carbon bonds, respectively.

[8] Allan, L. E. N.; Shaver, M. P.; White, A. J. P.; Gibson, V. C. *Inorg. Chem.*, in press.

[9] Wayland, B. B.; Poszmik, G.; Mukerjee, S. L.; Fryd, M. *J. Am. Chem. Soc.* **1994**, *116*, 7943.

[10] Davis, T. P.; Kukulj, D.; Haddleton, D. M.; Maloney, D. R. *Trends Polym. Sci.* **1995**, *3*, 7943.

[11] Debuigne, A.; Caille, J.-R.; Jérôme, R. *Angew. Chem., Int. Ed.* **2005**, *44*, 1101.

[12] Debuigne, A.; Caille, J.-R.; Detrembleur, C.; Jérôme, R. *Angew. Chem., Int. Ed.* **2005**, *44*, 3439.

[13] Debuigne, A.; Caille, J.-R.; Willet, N.; Jérôme, R. *Macromolecules* **2005**, *38*, 5452.

[14] Debuigne, A.; Caille, J.-R.; Willet, N.; Jérôme, R. *Macromolecules* **2005**, *38*, 9488.

[15] Grognec, E. L.; Claverie, J.; Poli, R. *J. Am. Chem. Soc.* **2001**, *123*, 9513.

[16] Stoffelbach, F.; Poli, R.; Richard, P. *J. Organomet. Chem.* **2002**, *663*, 269.

[17] Grishin, D. F.; Semyonycheva, L. L.; Telegina, E. V.; Smirnov, A. S.; Nevodchikovc, V. I. *Russ. Chem. Bull. Int. Ed.* **2003**, *52*, 505.

[18] Grishin, D. F.; Ignatov, S. K.; Shchepalov, A. A.; Razuvaev, A. G. *Appl. Organomet. Chem.* **2004**, *18*, 271.

[19] Braunecker, W. A.; Itami, Y.; Matyjaszewski, K. *Macromolecules* **2005**, *38*, 9402.

[20] Poli, R. *Angew. Chem., Int. Ed.* **2006**, *45*, 5058.

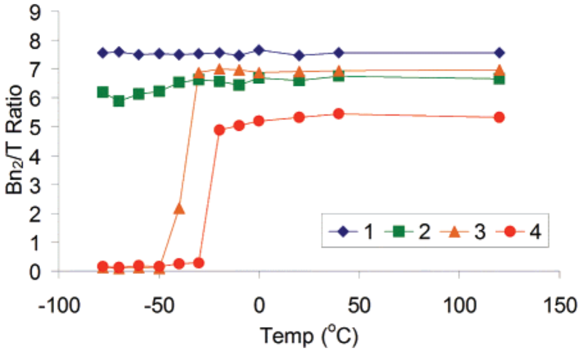

Figure 1. Ratio of integrated GC peaks for the formation of bibenzyl (Bn$_2$) and toluene (T) arising from the decomposition of $^{R',R''}$[*N*,*N*]FeCl$_2$Bn at different temperatures. Higher ratios indicate bibenzyl is the primary decomposition product. Ratios below 1 indicate toluene is the primary decomposition product.

Scheme 3. Decomposition of $^{Cy,R''}$[*N*,*N*]FeCl$_2$(CHMePh) Complexes

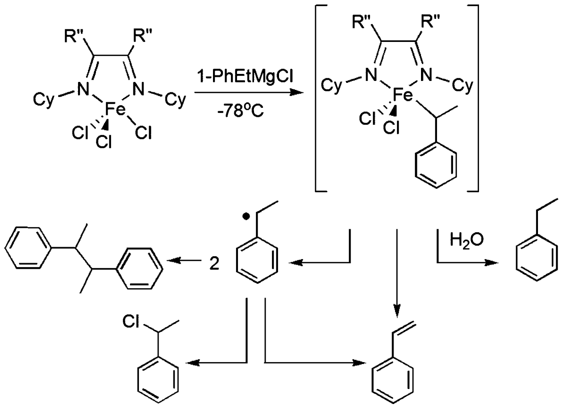

well with previously reported behavior for the intermediate spin-state complex ^{DiPP,H}[*N*,*N*]FeCl$_3$.[6]

Decomposition of these benzyl complexes does not reproduce the olefinic end-groups generated by catalytic chain transfer, however, since the $^{R',R''}$[*N*,*N*]FeCl$_2$Bn intermediates lack *β*-hydrogens. To more accurately reproduce the environment of a growing polystyrene chain, the study was extended to 1-phenylethyl iron complexes. Reaction of 1-phenylethyl magnesium chloride[21] with **1** or **3** in THF at −78 °C produced a slow color change to purple-brown, indicative of decomposition.

For both **1** and **3**, the major product was found to be 2,3-diphenylbutane, resulting from the coupling of two 1-phenylethyl radicals (**1**, 89%; **3**, 86%). In addition, styrene (**1**, 6%; **3**, 9%), ethylbenzene (**1**, **3**, 4%), and 1-phenylethyl chloride (**1**, **3**, 1%) were observed (Scheme 3). The formation of styrene confirms that olefin end-groups can be generated from Fe(III)-alkyl intermediates. The more carbophilic derivative **3** produces 50% more styrene than **1** during its decomposition. Increasing the concentration of Fe(II) species by “spiking” the reaction mixture with varying amounts of $^{Cy,R''}$[*N*,*N*]FeCl$_2$ during decomposition had no observable effect on the product distribution.

Trapping Experiments Using TEMPO. The organic radicals that form during the decomposition of $^{R',R''}$[*N*,*N*]FeCl$_2$R can be potentially trapped by other organic radical species. Decomposition of $^{Cy,F-Ph}$[*N*,*N*]FeCl$_2$(CHMePh) in the presence of tetramethylpiperidinyl-1-oxy (TEMPO) results in the formation of $^{Cy,F-Ph}$[*N*,*N*]FeCl$_2$ and 1-phenylethyl-substituted TEMPO, rather than 2,3-diphenylbutane, as shown in Scheme 4. The same product can alternatively be generated by mimicking the ATRP initiation step and reacting the Fe(II) complex with 1-phenylethyl chloride in the presence of TEMPO. This initiation reaction generates phenylethyl radicals with which the persistent TEMPO radical reacts.

Scheme 4. Trapping Alkyl Radicals Generated by Fe(III) Complex Decomposition and ATRP Initiation Reactions with TEMPO

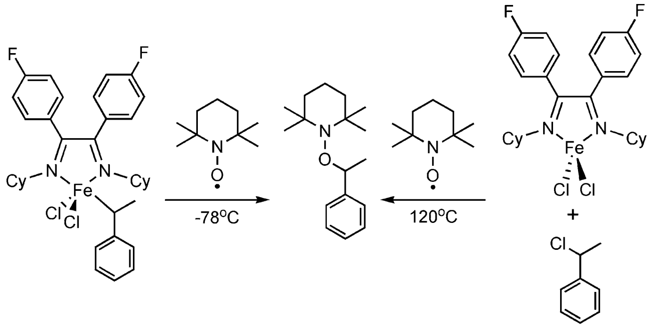

Table 1. OMRP of Styrene by α-Diimine Iron Catalysts[a]

catalyst	equiv	% conv	M_n	$M_{n,theo}$	PDI
none	0	100	7104	31 245	8.4
5	1.0	77	bimodal (shoulder)		
5	2.0	51	bimodal (shoulder)		
5	4.0	36	M_{pk1} ~50 000 M_{pk2} ~21 000		
5	8.0	24	bimodal (shoulder)		
6	1.0	48	16 117	14 998	3.7
6	2.0	31	12 001	9686	2.1
6	4.0	23	8268	7186	1.8
6	8.0	7.5	2190	2333	1.4

[a] AIBN, styrene, and catalyst equivalents of 0.5:300:X. Polymerizations conducted in sealed ampules at 120 °C in 1.0 mL of toluene for 48 h. Conversion of monomer determined by ^{1}H NMR. Molecular weights calculated by GPC versus styrene standards.

Organometallic-Mediated Radical Polymerizations (OMRP). If $^{R',R''}$[*N*,*N*]FeCl$_2$(P) species play a significant role in defining the chemistry of this system, initiation of a polymerization by a radical source such as AIBN (azobisisobutyronitrile) in the presence of $^{R',R''}$[*N*,*N*]FeCl$_2$ would be expected to establish the OMRP equilibrium independently of the ATRP equilibrium (see Scheme 1). We thus investigated a series of azo-initiated polymerizations using ^{Cy,H}[*N*,*N*]FeCl$_2$, **5**, and ^{DiPP,H}[*N*,*N*]FeCl$_2$, **6**, as catalyst precursors; the reactions were conducted at 120 °C in order to mimic the conditions of atom-transfer radical polymerization and to achieve efficient initiation of the polymerization. The results are collected in Table 1.

The polystyrene products generated using the high-spin system, **5**, were bimodal (Figure S2), appearing as shoulders for 1.0. 2.0, and 8.0 catalyst equivalents, but just resolved for 4.0 equiv. The latter revealed a M_{pk} for the higher molecular weight fraction of ca. 50 000 Da and ca. 21 000 Da for the lower molecular weight component. It is likely that the high molecular weight fraction is generated by bimolecular coupling of the radical chains, a termination process that would lead to doubling of the molecular weight. As the loading of **5** is increased relative to the radical initiator concentration, the lower molecular weight fraction increases proportionately, a consequence of more efficient trapping by the Fe(II) species; the low molecular weight fraction becomes dominant at 8 equiv of catalyst. The lower spin catalyst **6** gave monomodal distributions, and a decrease in polydispersity was observed with increasing catalyst loading,

---

[21] Baker, K. V.; Brown, J. M.; Hughes, N.; Skarnulis, A. J.; Sexton, A. *J. Org. Chem.* **1991**, *56*, 4585.

Table 2. OMRP of Styrene Catalyzed by α-Diimine Iron Complexes Using V-70 as Initiator[a]

catalyst	equiv	% conv	M_n	$M_{n,\text{theo}}$	PDI
none	0	100	8852	31 245	4.2
5	0.5	54	11 725	16 872	2.4
5	1.0	26	7297	8124	1.9
5	2.0	21	5953	6561	1.5
6	0.5	38	9681	11 873	2.0
6	1.0	20	5502	6249	1.5
6	2.0	12	3586	3749	1.3

[a] V-70, styrene, and catalyst equivalents of 0.5:300:X. Polymerizations conducted in sealed ampules at 70 °C in 1.0 mL of toluene for 48 h. Conversion of monomer determined by ^{1}H NMR. Molecular weights calculated by GPC versus styrene standards.

with moderate control (PDI = 1.4, $M_n = 2190$, $M_{n,\text{theo}} = 2333$) obtained using 8 equiv of catalyst. At these high temperatures the Fe(III)−R species is highly unstable and excessive catalyst loadings are required to obtain even moderate control. The reaction is extremely slow, with less than 10% conversion in 48h. It is apparent that the α-diimine iron complexes can operate in OMRP equilibria to control the polymerization, but under these high-temperature conditions they are not particularly effective catalysts.

Since the iron-alkyl species should be more stable at lower temperatures, 2,2′-azobis(4-methoxy-2,4-dimethylvaleronitrile), V-70, with a half-life of 10 h at 30 °C, was investigated. The results of screening reactions at 70 °C are shown in Table 2. Control over the polymerization is now achievable using 2 equiv of catalyst, with lower spin **6** displaying narrower molecular weight distributions than for its high-spin relative **5**.

Further Studies. A series of further experiments was carried out to help elucidate the interplay of the ATRP and OMRP equilibria.

Mixed Catalyst Systems. The effect of mixing an efficient ATRP catalyst with a catalyst that promotes termination through CCT should allow control over the rate of polymerization and molecular weight of the polymer produced. Conducting styrene polymerizations with catalyst mixtures comprising the ATRP-directing catalyst, $^{\text{Cy,H}}[N,N]\text{FeCl}_2$ **5**, and the CCT-directing catalyst, $^{\text{Cy,F-Ph}}[N,N]\text{FeCl}_2$ **7**, in ratios of 9:1, 3:1, and 1:1 showed that an increased concentration of **7** both decreases the rate (10% **7**, 0.20 h^{-1}; 25% **7**, 0.09 h^{-1}; 50% **7**, 0.06 h^{-1}; Figure S7 in the SI) and lowers the molecular weight of the resultant polymer. As the concentration of CCT catalyst increases, molecular weight distributions develop a pronounced tailing toward lower molecular weights (Figure S8 in the SI) and can be attributed to an increase in the proportion of chain-transfer events. Consistently, ^{1}H NMR studies showed a 5-fold increase in the number of olefin-terminated polymer chains as the catalyst ratio is changed from 9:1 to 1:1.

Catalyst Loading. In classic CCT systems, doubling the concentration of catalyst maintains a similar rate but decreases the molecular weight of the short-chain oligomers.[22−24] Doubling the concentration of $^{\text{Cy,F-Ph}}[N,N]\text{FeCl}_2$, **7**, doubled the rate of the reaction but did not change the molecular weight of the resultant polymer.

Discussion

Organometallic Intermediates. The alkylation/decomposition experiments and organometallic-mediated radical polymerization studies highlight the potential involvement of $^{\text{R}',\text{R}''}[N,N]\text{FeCl}_2(\text{P})$ species during atom-transfer radical polymerizations of styrene. The Fe(III)-alkyl stability studies clearly demonstrate a correlation between iron−carbon bond strength and the spin-state of the Fe(III) complexes. High-spin ($S = 5/2$) Fe(III)-alkyl species are unstable at −78 °C, while the substitution of an electron-withdrawing aryl group at the 2,3 position gives improved thermal stability to the alkyl species and correlates with a lowering of the Fe(III) spin-state. These intermediate spin-state complexes are more efficient alkyl radical traps and correlate with a switch to catalytic chain transfer as the observed chain termination mechanism. To date, despite repeated attempts, it has not proven possible to isolate and characterize an Fe(III)-alkyl species.

Studies under OMRP conditions show that catalysts **5**−**7** can engage in OMRP equilibria, but that they are not particularly effective catalysts for the OMRP of styrene due to the low stability of the Fe(III)-alkyl species under the high-temperature conditions of the polymerization. Employing AIBN as an initiating system at 120 °C, 8 equiv of catalyst are required to afford moderate control. Nevertheless, a spin-state effect is observed, with ligands favoring lower spin-state Fe(III) centers acting as superior catalysts. With V-70, the polymerizations can be performed at lower temperatures and with lower catalyst loadings.

Organoradical-Trapping/*β*-Hydrogen Elimination versus Direct Hydrogen Transfer. An issue for the OMRP process is the mechanism of chain transfer, which may proceed either via direct H atom abstraction from the organoradical or via initial formation of an Fe(III)-alkyl species followed by *β*-hydrogen elimination to give the unsaturated polymer product. In the decomposition studies of 1-phenylethyliron complexes, the lower spin carbophilic catalyst, $^{\text{Cy,F-Ph}}[N,N]\text{FeCl}_3$, generates 50% more styrene than its high-spin relative. If the $^{\text{R}',\text{R}''}[N,N]\text{FeCl}_2\text{R}$ complex has a longer lifetime due to increased carbophilicity of the parent catalyst, decomposition through *β*-H elimination would be expected to generate more styrene. Conversely, a direct hydride-transfer mechanism should not depend upon Fe−R stability, but rather on Fe(II) concentration. Addition of $^{\text{Cy,F-Ph}}[N,N]\text{FeCl}_2$, **7**, to the reaction mixture prior to complex decomposition did not affect the amount of styrene formed, suggesting that the organometallic pathway is favored. Further, the doubling of the rate of polymerization upon doubling of catalyst concentration but with no change in the polymer molecular weight suggests that this system does not operate via a traditional H-transfer CCT mechanism. In our case, the rate of reaction would increase due to a shift in the ATRP equilibrium and an increase in radicals in solution, while the organometallic complexes formed would also double in concentration. Since both monomer consumption and termination rates are doubled, the observed molecular weight remains the same. Together, these observations lend support to an organoradical-trapping/*β*-hydrogen elimination pathway.

Effect of the OMRP Equilibrium on the Overall Outcome of the Polymerization. The moderate control over styrene polymerization under OMRP conditions confirms the likely involvement of trapped alkyl radicals in ATRP equilibria. In all cases, however, control of the polymerization by the carbophilic regime is mediocre at best. In many ways, this is expected since, regardless of their substituents, Fe(III)-alkyl complexes decompose at low temperatures (−30 °C) and therefore will have a short half-life under ATRP reaction conditions (120 °C). With the OMRP equilibrium shifted toward the Fe(II) species, the radical concentration remains high and

---

(22) Enikolopyan, N. S.; Smirnov, B. R.; Ponomarev, G. V.; Bel'govskii, I. M. *J. Polym. Sci. Polym. Chem. Ed.* **1981**, *19*, 879.

(23) Burczyk, A. F.; O'Driscoll, K. F.; Rempel, G. L. *J. Polym. Sci. Polym. Chem. Ed.* **1984**, *22*, 3255.

(24) Gridnev, A. A.; Ittel, S. D.; Fryd, M.; Wayland, B. B. *Organometallics* **1993**, *12*, 4871.

Table 3. Radical Concentrations for ATRP and OMRP of Styrene with Various Catalysts

entry	R′	R″	k_{app} (s^{-1})	[$R^\bullet$]	mechanism
1	Cy	NMe_2-Ph	2.00×10^{-4}	9.80×10^{-8}	ATRP
2	Cy	H	6.83×10^{-5}	3.34×10^{-8}	ATRP
3	Cy	Me	4.67×10^{-5}	2.28×10^{-8}	ATRP/CCT
4	Cy	MeO-Ph	2.83×10^{-5}	1.39×10^{-8}	ATRP/CCT
5	DiPP	H	1.39×10^{-5}	6.79×10^{-9}	CCT
6	Cy	Me-Ph	1.17×10^{-5}	5.71×10^{-9}	CCT
7	Cy	Ph	9.44×10^{-6}	4.62×10^{-9}	CCT
8	Cy	F-Ph	6.11×10^{-6}	2.99×10^{-9}	CCT
9	Cy	H	1.67×10^{-6}	3.47×10^{-9}	OMRP
10	DiPP	H	1.53×10^{-6}	3.18×10^{-9}	OMRP

control is lost without very high levels of catalyst loading and lower reaction temperatures. But if poor carbophilicity persists across the substitution patterns studied, why does such a drastic switch in mechanism occur?

Under ATRP conditions, halogen- and olefin-terminated polymer products are formed because of differences in the *relative* halogeno- versus carbophilicities of the various α-diimine iron catalysts. These effects become apparent upon inspection of the radical concentrations, which are controlled by both the halogenophilic and carbophilic equilibria operating under ATRP conditions. The concentration of radicals is related to the apparent rate constant by eq 1, where k_{app} is the apparent rate constant for the polymerization and k_p is the propagation rate constant for styrene at a temperature T. Values for [$R^\bullet$] with different α-diimines under ATRP and OMRP conditions are tabulated in Table 3.

$$k_{app} = k_p[R^\bullet] \text{ where } k_p = 10^{7.630} \text{ L mol}^{-1} \text{ s}^{-1} \text{ e}^{(-32.51 \text{ kJ/mol}/RT)} \quad (1)$$

Entries 1−8 draw upon kinetic runs described in previous papers in this series.[8,25,26] A correlation between radical concentration and polymerization mechanism is readily apparent. Increased electron donation from the α-diimine ligand leads to greater concentrations of radicals and, thus, markedly faster polymerization rates. In entries 1 and 2, the consumption of monomer is fast relative to chain-transfer reactions, and classic ATRP behavior is observed. A decrease in [$R^\bullet$] and k_{app} slows monomer consumption; in these cases, catalytic chain-transfer events become kinetically competitive, and evidence for both mechanisms is observed. When the polymerization rate is slowed to a sufficient extent, catalytic chain-transfer events dominate and short-chain, olefin-terminated polymers are observed. The change from ATRP to CCT behavior is not abrupt, but rather a consequence of a gradual decrease in k_{app} relative to the chain-transfer reaction. This gradual switch in polymerization mechanism is reproduced by mixed catalyst systems consisting of $^{Cy,H}[N,N]FeCl_2$, **5**, and $^{Cy,F-Ph}[N,N]FeCl_2$, **7**. Increasing the proportion of **7**, a catalyst with decreased halgenophilicity and increased carbophilicity, leads to lower rates and lower radical concentrations. As chain-transfer termination reactions increase, the molecular weights decrease and the distributions show pronounced tailing toward low molecular weights.

Comparing the radical concentrations in Table 3 for catalysts operating in the ATRP and OMRP regimes reveals that OMRP radical concentrations are not significantly different from those observed under ATRP conditions. Relatively minor differences exist between radical concentrations for cyclohexylimino catalysts and 2,6-diisopropylphenylimino catalysts under OMRP conditions (entries 9, 10, respectively), compared to an 8-fold increase in [$R^\bullet$] under ATRP/CCT conditions (entries 2 versus 5). Thus, the difference in *carbophilicity* between these two catalysts, though discernible, is not all that significant, and therefore we conclude that carbophilicity *per se* does not account for the observed change in mechanism. Rather, the change in spin-state of the parent Fe(III) complexes must induce a more drastic change in *halogenophilicity*, and it is this effect that leads to the more profound influence on mechanistic pathway.

The organometallic (OMRP) pathway alone is unable to control the polymerization because most of the control is derived from the atom-transfer equilibrium. As illustrated in Scheme 1, the radical-trapping equilibrium disfavors the unstable Fe(III)-alkyl complex, keeping the radical concentration high unless excessive catalyst loadings are used. This organometallic pathway, though not dominant, provides a route to catalytic chain transfer. Decreased halogenophilicity is provided by electron-withdrawing groups on the catalyst backbone and is "switched on" by a change in spin-state of the parent Fe(III) complexes; under ATRP conditions, the polymerization slows and causes the termination event to be kinetically competitive, generating CCT products. The α-diimine iron catalysts effectively control the polymerization through the ATRP equilibrium, while the OMRP equilibrium provides a link between halogen-terminated and olefin-terminated polymer products.

Conclusions

The contrasting ATRP versus CCT behavior of $^{R',R''}[N,N]$-$FeCl_2$ catalysts correlates strongly with the spin-state of the oxidized Fe(III) species and can be explained by the differing halogeno- versus carbophilicities of the iron centers in these Fe(II) complexes. Studying the decomposition of Fe(III) benzyl and 1-phenylethyl complexes showed increased stability for systems derived from Fe(III) complexes that are intermediate spin in character, and these systems favor CCT. Azo-initiated polymerizations of styrene (under OMRP conditions) are moderately controlled by these α-diimine iron catalysts. While the observed mechanism (ATRP versus CCT) strongly correlates with metal spin-state of the Fe species, the rate of the polymerization and nature of the polymer produced is dependent upon the radical concentration generated by the competing OMRP and ATRP equilibria. Halogenophilic catalysts, i.e., those possessing electron-donating substituents, afford increased rates of monomer consumption and increased control via ATRP; the chain-transfer reaction is not kinetically relevant under these circumstances. Conversely, catalysts bearing electron-withdrawing groups have decreased halogenophilicity, resulting in slower rates of monomer consumption and the observation of unsaturated polymer chains arising from chain transfer.

Experimental Section

General Experimental Procedures. All manipulations of air- and/or moisture-sensitive compounds were carried out under nitrogen using standard Schlenk and cannula techniques or in a conventional nitrogen-filled glovebox. NMR spectra were recorded on a Bruker AV-400 (^{1}H, 400.3 MHz; ^{13}C, 100.7 MHz) spectrometer, at 293 K unless stated otherwise. Chemical shifts are reported as δ (in ppm) and referenced to the residual proton signal and to the ^{13}C signal of the deuterated solvent, respectively; coupling constants are reported in Hz. The following abbreviations have been used for multiplicities: s (singlet), d (doublet), t (triplet), m (unresolved multiplet), br (broad). GC analyses were conducted on an Agilent 6890A gas chromatograph with a HP-5 column. GC/CI (chemical ionization) or EI (electron impact) mass spectra were

---

[25] Gibson, V. C.; O'Reilly, R. K.; Reed, W.; Wass, D. F.; White, A. J. P.; Williams, D. J. *Chem. Commun.* **2002**, 1850.

[26] O'Reilly, R. K.; Shaver, M. P.; Gibson, V. C.; White, A. J. P. Submitted to *Macromolecules.*

recorded on either a VG Autospec or a VG Platform II spectrometer at Imperial College London. GPC data were collected using Cirrus GPC/SEC software, version 1.11, connected to a Shodex RI-101 detector, and were referenced to polystyrene standards (Polymer-Labs EasiCal, PS1). Solvents were dried by refluxing over an appropriate drying agent and distilling, or passing through a cylinder filled with commercially available Q-5 catalyst (13% Cu(I) oxide on Al_2O_3) and activated Al_2O_3 (3 mm, pellets) in a stream of nitrogen, and were degassed before use. NMR solvents were dried over molecular sieves and degassed prior to use. Styrene was stirred over calcium hydride for 24 h, vacuum-transferred, degassed, and then stored in an inert atmosphere at −35 °C. ${}^{R',R''}[N,N]FeCl_2$ catalysts **5**−**7** were prepared according to literature procedures.[6,25,27] ${}^{R',R''}[N,N]FeCl_3$ precursors **1**−**4** were prepared according to literature procedures,[6,8] stored in the absence of light, and used within 1 week of synthesis. $C_6H_5CHMeMgCl$ was synthesized according to a literature procedure.[21] AIBN was purchased from Aldrich Chemical Co., stored at −35 °C, and used as received. V-70 was purchased from Wako Chemicals Company, stored at −35 °C, and used as received. All other reagents were purchased from ACROS Organics or Aldrich Chemical Co. and used as received.

General Procedure for Alkyl Decomposition Experiments. ${}^{R',R''}[N,N]FeCl_3$ (0.500 mmol) was dissolved in THF (10 mL) and cooled to −78 °C. Dropwise addition of a solution of RMgCl (0.500 mmol) in THF resulted in the precipitation of a white solid ($MgCl_2$). An aliquot (1 mL) was removed from the reaction mixture and quenched with distilled H_2O. Subsequent aliquots were removed and quenched over a range of temperatures. Depending on the stability of the corresponding alkyl complex, vivid color changes corresponding to the formation of ${}^{R',R''}[N,N]FeCl_2$ were observed at various temperatures on warming. Aliquots were filtered through basic alumina and analyzed by GC or GC/MS. GC area counts were corrected against organic components present in unreacted RMgCl.

Reaction of ${}^{Cy,F-Ph}[N,N]FeCl_2(CHMePh)$ with TEMPO. ${}^{Cy,F-Ph}[N,N]FeCl_3$ (0.500 mmol) was dissolved in THF (10 mL) and cooled to −78 °C. A solution of TEMPO (0.500 mmol) in THF (5 mL) was added to this mixture dropwise via cannula and an aliquot removed from the reaction. Addition of 1-PhEtMgCl (0.500 mmol) in THF resulted in the precipitation of a white solid ($MgCl_2$). The reaction mixture was warmed to room temperature and quenched with degassed H_2O. The organic fraction was separated, filtered through alumina, dried *in vacuo*, and recrystallized from Et_2O to yield 1-(benzyloxy)-2,2,6,6-tetramethylpiperidine as a white solid in 61% yield. ^1H NMR ($CDCl_3$): δ 1.02, 1.16, 1.29, 1.31 (4 × 3H, s, CH_3), 1.46−1.56 (6H, m, CH_2), 1.77 (3H, d, $^3J_{H-H}$ 6.4, CH_3-CH), 4.77 (1H, q, $^3J_{H-H}$ 6.4, CH-CH_3), 7.22−7.31 (5 H, m, Ar-*H*). ^{13}C NMR ($CDCl_3$): δ 15.9, 18.4, 23.2, 24.1, 25.6, 25.8, 34.1, 48.9, 78.1, 140.7, 126.5, 128.4, 129. MS (EI$^+$, *m*/*z*): 261 [M$^+$].

Reaction of ${}^{Cy,F-Ph}[N,N]FeCl_2$ with 1-PECl and TEMPO. To an ampule equipped with a magnetic stirrer bar were added toluene (3 mL), ${}^{Cy,H}[N,N]FeCl_2$ (0.100 mmol), 1-phenylethyl chloride (0.100 mmol), and TEMPO (0.100 mmol). The ampule was then sealed and heated in a sand bath at 120 °C for 1 h. The ampule was then removed from heat and the contents were dissolved in THF, filtered through alumina, dried *in vacuo*, and recrystallized from Et_2O to afford 1-(1-phenylethoxy)-2,2,6,6-tetramethylpiperidine in 56% yield. ^1H NMR ($CDCl_3$): δ 1.02, 1.16, 1.29, 1.31 (4 × 3H, s, CH_3), 1.46−1.56 (6H, m, CH_2), 1.77 (3H, d, $^3J_{H-H}$ 6.4, CH_3-CH), 4.77 (1H, q, $^3J_{H-H}$ 6.4, CH-CH_3), 7.22−7.31 (5 H, m, Ar-*H*). ^{13}C NMR ($CDCl_3$): δ 15.9, 18.4, 23.2, 24.1, 25.6, 25.8, 34.1, 48.9, 78.1, 140.7, 126.5, 128.4, 129. MS (EI$^+$, *m*/*z*): 261 [M$^+$].

General Procedure for Polymerization Screening. All polymerizations were set up and performed under an atmosphere of oxygen-free, dry nitrogen using standard Schlenk-line and glovebox techniques. To an ampule equipped with a magnetic stirrer bar was added a solution of monomer, solvent (where applicable) initiator, and catalyst and then sealed. In most cases the catalyst was soluble in the monomer solution. The ampules were heated in an oil or sand bath at 70 or 120 °C for an allotted period of time. Aliquots (0.3 mL) were removed at appropriate intervals. Conversion was determined by integration of the monomer versus polymer backbone resonances in the ^1H NMR spectrum of the crude product in $CDCl_3$. The polystyrene was dissolved in THF and precipitated into acidified methanol, filtered, and washed with methanol. The precipitate was collected and dried for 24 h under vacuum. Samples were then analyzed by GPC.

Acknowledgment. The authors thank the Natural Sciences and Engineering Research Council of Canada for a postdoctoral fellowship (to M.P.S.) and the Engineering and Physical Sciences Research Council (UK) for a studentship (to L.E.N.A.).

Supporting Information Available: Tables of GC product distributions for alkylation experiments and tables and plots for the organometallic-mediated radical polymerization of styrene. This material is available free of charge via the Internet at http://pubs.acs.org.

OM700395H

---

(27) Gibson, V. C.; O'Reilly, R. K.; Wass, D. F.; White, A. J. P.; Williams, D. J. *Macromolecules* **2003**, *36*, 2591.